doi:10.1016/j.jmb.2009.09.056 J. Mol. Biol. (2009) 394, 627–633

JMB

Available online at www.sciencedirect.com

ScienceDirect

ELSEVIER

COMMUNICATION

Binding Modes of Thioflavin-T to the Single-Layer β-Sheet of the Peptide Self-Assembly Mimics

Chun Wu[1], Matthew Biancalana[2], Shohei Koide[2]* and Joan-Emma Shea[1,3]*

[1]*Department of Chemistry and Biochemistry, University of California, Santa Barbara, CA 93106, USA*

[2]*Department of Biochemistry and Molecular Biology, University of Chicago, 929 East 57th Street, Chicago, IL 60637, USA*

[3]*Department of Physics, University of California, Santa Barbara, CA 93106, USA*

Received 1 July 2009; received in revised form 18 September 2009; accepted 23 September 2009
Available online 30 September 2009

Edited by D. Case

Although the amyloid dye thioflavin-T (ThT) is among the most widely used tools in the study of amyloid fibrils, the mechanism by which ThT binds to fibrils and other β-rich peptide self-assemblies remains elusive. The development of the water-soluble peptide self-assembly mimic (PSAM) system has provided a set of ideal model proteins for experimentally exploring the properties and minimal dye-binding requirements of amyloid fibrils. PSAMs consist of a single-layer β-sheet (SLB) capped by two globular domains, which capture the flat, extended β-sheet features common among fibril-like surfaces. Recently, a PSAM that binds to ThT with amyloid-like affinity (low micromolar K_d) has been designed, and its crystal structure in the absence of bound ThT was determined. This PSAM thus provides a unique opportunity to examine the interactions of ThT with a β-rich structure. Here, we present molecular dynamics simulations of the binding of ThT to this PSAM β-sheet. We show that the primary binding site for ThT is along a shallow groove formed by adjacent Tyr and Leu residues on the β-sheet surface. These simulations provide an atomic-scale rationale for this PSAM's experimentally determined dye-binding properties. Together, our results suggest that an aromatic–hydrophobic groove spanning across four consecutive β-strands represents a minimal ThT binding site on amyloid fibrils. Grooves formed by aromatic–hydrophobic residues on amyloid fibril surfaces may therefore offer a generic mode of recognition for amyloid dyes.

Keywords: amyloid; thioflavin-T; cross-β; binding; molecular dynamics simulation

Thioflavin-T (ThT) is one of the most commonly used fluorescent dyes to study the kinetics of fibrillization and to stain amyloid plaques.[1,2] ThT's fluorescence emission is dramatically enhanced upon fibril binding, which makes ThT particularly useful in real-time detection of fibrils. ThT does not typically bind to monomeric proteins but appears to recognize and bind to some inherent structural features of amyloid fibrils. An atomic characterization of the binding sites of ThT to fibrils is severely hampered by the non-crystalline nature of fibrils. To date, no high-resolution structures of ThT bound to β-rich, fibril-like materials have been determined.

In an attempt to overcome this experimental limitation, Koide and coworkers have recently developed the peptide self-assembly mimic (PSAM) platform, an engineered system in which a single β-sheet is covalently capped by two soluble protein domains.[3] This system reproduces some of the main structural features of a fibril, a flat single-layer β-sheet (SLB) made of repeats of a short peptide building block (Fig. 1b), while being amenable to crystallization and solution-state biophysical analyses. The

**Corresponding authors.* J.-E. Shea is to be contacted at the Department of Chemistry and Biochemistry, University of California, Santa Barbara, CA 93106, USA. E-mail addresses: shea@chem.ucsb.edu; skoide@uchicago.edu.

Abbreviations used: ThT, thioflavin-T; PSAM, peptide self-assembly mimic; SLB, single-layer β-sheet; PEG, polyethylene glycol; MD, molecular dynamics; MM-GBSA, molecular mechanics-generalized Born/surface area.

wild-type PSAM contains primarily charged or polar residues on its surface and shows no detectable binding to ThT—hence, this PSAM served as an excellent inert scaffold in which a ThT-binding site could be designed.

Because it has been suggested that hydrophobic residues, particularly aromatic amino acids, form especially favorable sites for amyloid dye binding,[7,14] Biancalana *et al.* examined a number of PSAM mutants with various combinations of

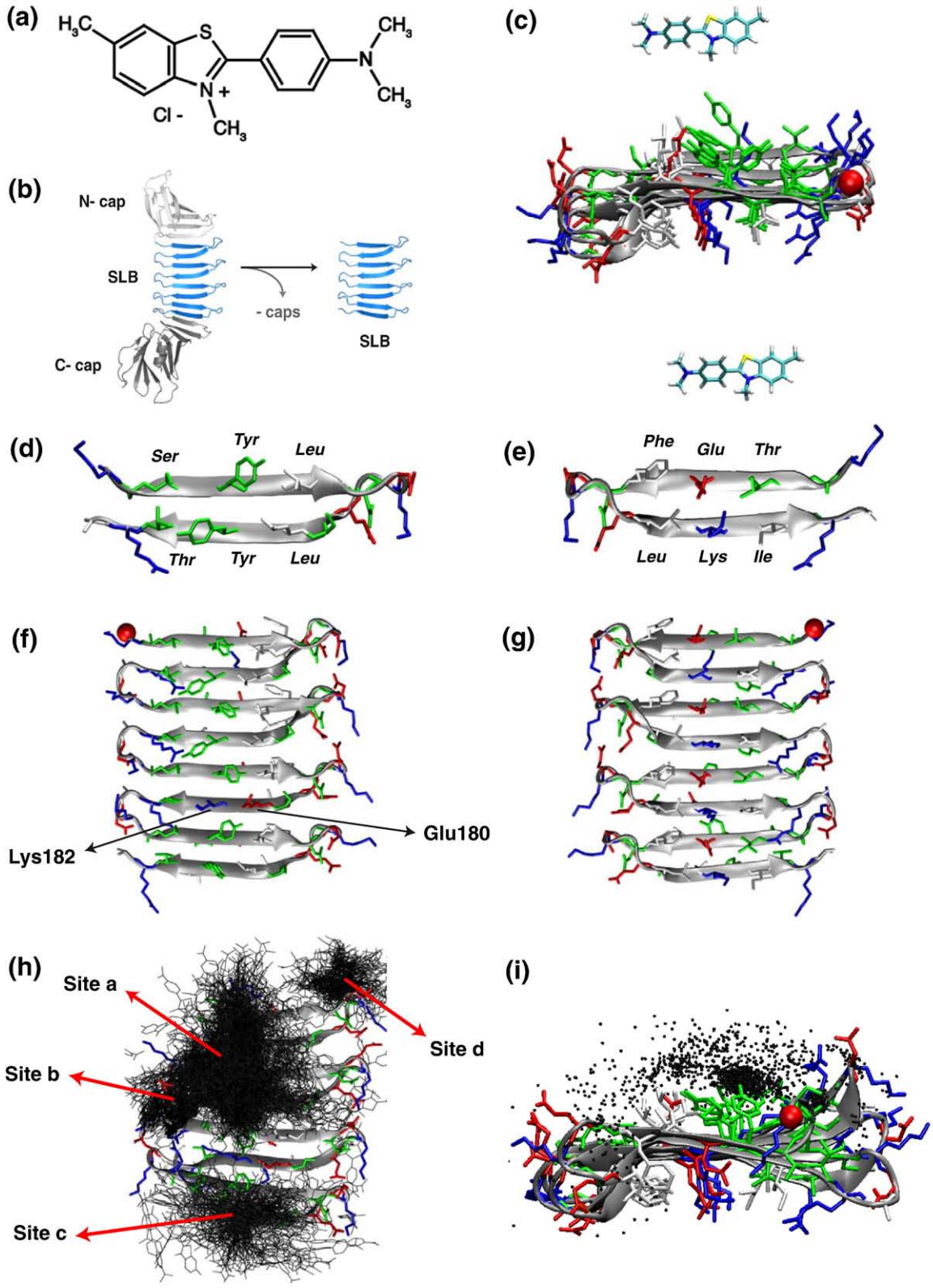

Fig. 1 *(legend on next page)*

consecutive apolar and aromatic residues to identify the minimum requirements (length and side-chain type) for ThT binding.[4] These mutations were introduced onto one face of the SLB as parts of "cross-strand ladders," which are formed from repetitive rows of side chains running perpendicular to the β-strands. The ladder motif is a general property of all fibril-like structures formed from the self-assembly of short β-rich polypeptides and has been implicated as a key recognition motif for fibril-binding dyes.[15]

This minimalist design led to the finding that the 5-YY/LL PSAM (which possesses consecutive Tyr and Leu in adjacent ladders across five β-strands) recapitulated a micromolar K_d binding-site characteristic of true amyloid (as measured by ThT fluorescence).[4] The crystal structure of 5-YY/LL revealed that the adjacent Tyr and Leu ladders formed a shallow groove that was large enough to accommodate a single ThT molecule. Unfortunately, despite the addition of >10× molar excess of ThT to the crystallization conditions, ThT electron density was not observed. Biancalana *et al.* hypothesized that the polyethylene glycol (PEG) 400 used in the crystallization prevented binding of ThT, as evidenced by lack of ThT fluorescence in the presence of the precipitant. Moreover, electron density was observed for two PEG 400 molecules along the Tyr groove, suggesting direct competition between ThT and PEG 400 for binding to the ladder side chains. Further attempts to study the binding of ThT to the PSAM via solution NMR were unsuccessful due to extensive overlap of resonances and the large size of the molecule. In this article, we use molecular dynamics (MD) simulations to elucidate the binding of ThT to the 5-YY/LL PSAM system.

We considered only the SLB (residues 119–209) of the 5-YY/LL PSAM crystal structure (Protein Data Bank ID: 3EC5)[4] in our binding simulations to two ThT molecules (see Fig. 1a–g). The SLB of the 5-YY/LL PSAM contains four homologous β-hairpins with a total of eight β-strands. The N- and C-terminal globular domains (residues 27–118 and 209–342) of the PSAM were not included in the simulation, as it has been experimentally demonstrated that ThT does not bind to either in a mode that enhances its fluorescence emission. Moreover, such capping groups would not be seen in a typical amyloid fibril. Exclusion of the globular domains improves computational efficiency and also allows us to explore the hypothetical binding of ThT to the uncapped β-strands of the SLB (mimicking binding to the terminal edge of a fibril). Details of the system and the binding simulations are given in the caption of Fig. 1.

Fig. 1. Binding of ThT to the SLB of the 5-YY/LL PSAM. (a) Structure of ThT. (b) The PSAM consists of a single β-sheet covalently capped by two soluble protein domains. The N- and C-terminal caps of the 5-YY/LL PSAM were omitted in our simulations. (c) The initial conformation of the SLB with two ThT molecules. (d) The aromatic–hydrophobic surface showing three adjacent pairs of protruding cross-strand residues (Ser-Thr, Tyr-Tyr/YY, and Leu-Leu/LL) of the repeating β-hairpin unit in SLB. (e) The charged surface showing three adjacent pairs of protruding residues (Phe-Leu, Glu-Lys, and Thr-Ile) of the repeating β-hairpin unit in the SLB. (f) The aromatic–hydrophobic surface showing the five cross-strand Tyr side chains 5-YY/LL ladder. (g) The charged surface showing charged residues (Lys and Glu) of the SLB. (h) Dominant binding of ThT on the aromatic–hydrophobic surface (e.g., containing the Tyr and Leu ladder). Four clusters are located: at the shadow groove formed by the continuous five Tyr side chains, on top of β-strands 3–5, and at two edges of the SLB (sites a–d). ThT molecules are represented by lines. (i) Lateral view: almost no binding on the charged surface of the SLB (each black dot represents a ligand). The N-terminus of the SLB is shown as a red ball. The positively charged, negatively charged, and hydrophobic side chains of the peptide are colored blue, red, and black, respectively. Atoms C, N, S, and H of the dye are colored cyan, blue, yellow, and white, respectively. *System preparation*: The binding simulation consisted of the SLB (residues 119–209) of the 5-YY/LL PSAM β-sheet (Protein Data Bank ID: 3EC5)[4], two ThT molecules, 5639 water molecules, and two chloride ions. The two ThT dye molecules were initially placed ~10 Å away from the β-sheet along the normal direction to the β-sheet surface. The two negative chloride ions (Cl^-) were added to neutralize the positive charges carried by the ThT molecules. The solute molecules were immersed into a rectangular box with dimensions of 64 Å × 60 Å × 63 Å. The periodic water box was constructed in such a way that the solute was at least ~8 Å away from the box surface, and the minimum distance between the solute and the image was ~16 Å. The Duan *et al.* all-atom point-charge force field[5] (AMBER ff03) was chosen to represent the polypeptide. The solvent was explicitly represented by the TIP3P[6] water model. The parameters for ThT were obtained from a previous study[7] and are attached in AMBER force field file format. *Binding simulations*: The AMBER 8 simulation package[8] was used in both MD simulations and data processing. The ligand–protein–water system was subjected to periodic boundary conditions via both minimum image and discrete Fourier transform as part of the particle-mesh Ewald method.[9] After the initial energy minimization, a total of five simulations were performed with different initial random velocities. The initial velocities were generated according to the Maxwell–Boltzmann distribution at 500 K. The simulations started after a 10.0-ps run at 500 K to randomize the orientations and positions of the two ThT dye molecules. A short 1.0-ns MD at 310 K in the NPT ensemble (constant pressure and temperature) was performed to adjust system size and density and to equilibrate the solvent. The simulations were continued at 310 K for 99 ns in the NVT ensemble (constant volume and temperature). The elevated temperature (10 K higher than 300 K) was used in the simulations to enhance the hydrophobic effect. Particle-mesh Ewald method[9] was used to treat the long-range electrostatic interactions. SHAKE[10] was applied to constrain all bonds connecting hydrogen atoms, and a time step of 2.0 fs was used. In order to reduce the computation, we calculated non-bonded forces using a two-stage RESPA approach[11] where the forces within a 10-Å radius were updated every step and those beyond 10 Å were updated every two steps. The Langevin dynamics was used to control the temperature (310 K) using a collision frequency of 1.0 ps^{-1}. The lower collision frequency than a typical value (~60 ps^{-1}) for water solvent was used for a better conformational sampling. The center of mass translation and rotation were removed every 500 steps. Studies have shown that this removes the "block of ice" problem.[12,13] The trajectories were saved at 2.0-ps intervals for further analysis. Forty Xeon 64-bit processors (2.66 GHz) were used for ~60 days to complete the five binding simulations.

The SLB of the 5-YY/LL PSAM retained its β-sheet structure and was stable at 310 K over the course of all five 100.0-ns binding simulations, as indicated by the small C^{α} root-mean-square distance (2.9± 0.6 Å) from the starting crystal structure. The small structural fluctuations observed in the simulations arose primarily from subtle twisting and bending of the SLB, in agreement with conformational variations seen in a series of PSAM crystal structures and in solution NMR spectroscopy data.[3] The convergence of the simulations was confirmed by many reversible binding events of dye molecules to the β-sheet (Fig. S1).

To identify the binding sites of the dye, we superimposed the β-sheet structure of the bound complexes identified from the trajectories (Fig. 1h and i). Most of ThT binding is located on the β-sheet face of 5-YY/LL into which the ladder mutations of Tyr and Leu were introduced (referred to as the "aromatic–hydrophobic" face hereafter; Fig. 1f and h). Four populated dye clusters are identified (Fig. 1h): the biggest cluster is in the shallow groove formed by the five consecutive Tyr side chains; the second cluster is on β-strands 3–5 (numbered from N- to C-terminus); the other clusters are at the two edges of the β-sheet. The dominant binding site along the Tyr residues coincides with the proposed site from the experimental study.[4] In contrast, almost no binding was observed on the opposite, "charged" face of the β-sheet, which contains numerous Lys and Glu charge pairs across β-strands (Fig. 1i). Binding to the aromatic–hydrophobic surface is also interrupted by charged residues (Glu180 and Lys182) on the sixth β-strand (Fig. 1g). These data are consistent with the experimental observation that ThT does not appreciably bind to the highly charged wild-type PSAMs[4] and highly charged fibrils. Indeed, Biancalana *et al.* showed that a single point mutation of either Tyr or Leu to Lys at the two corners of the YY/LL ladders dramatically reduced ThT binding.[4] Our simulations suggest that this decrease in binding affinity is likely due to positive charge repulsion between the ThT and Lys moieties.

To gain a clearer understanding of the binding interactions, we grouped the bound complexes into different structural families based on the RMSD of the dye molecule (cutoff of 5 Å), after aligning the SLB.[16] A representative structure (the centroid) of the top 26 structural families from the combined five simulation runs is shown in Fig. S2. The top 26 structural families of the bound complex were grouped into four superfamilies based on the four binding sites described earlier. The representative complex structure for each superfamily is shown in Fig. 2.

ThT binding on top of the Tyr side chains, as observed in the dominant mode A, appears to be the most favorable interaction with the 5-YY/LL SLB, as indicated by the greater abundance seen in the clustering studies (59% for mode A *versus* 19%, 8%, and 6% for modes B, C, and D, respectively; Fig. 2). In mode A, the two conjugated rings of ThT pack extensively against the continuous Tyr surface, contributing a number of hydrophobic and aromatic stacking interactions. Additionally, several hydrophobic contacts between the aromatic rings and methyl groups of ThT are mediated by the adjacent Leu ladder. The benzathiole ring tends to lay parallel with the β-sheet surface, exposing the positively charged nitrogen to the solvent (Fig. 2a). This arrangement prevents burial of the charged moiety in hydrophobic Tyr surface, thus avoiding a desolvation penalty upon binding.

Though the orientations of the ThT molecules bound in site A are parallel, they are dispersed by a longitudinal translation across the five Leu and Tyr residues with a magnitude up to the spacing between adjacent β-strands (see Fig. S2, A1–A16). The lack of a single, well-defined position of bound ThT within site A indicates that the groove formed by the five cross-strand residue pairs is slightly longer than the minimal ThT binding site. Indeed, the length of ThT (~15 Å) more accurately reflects the spacing between four cross-strand residues (~14 Å) than between five (~19 Å), suggesting that this slightly smaller site comprises a truly minimal ThT binding motif in the PSAM. Although Biancalana *et al.* have shown that a PSAM containing a 4-YY/LL ladder does not appreciably bind ThT, this effect is likely to have been caused by the particular choice of charged amino acids (Lys and Glu) to replace the Tyr and Leu residues.[4] Indeed, as we have shown in this work, Lys and Glu strongly repel ThT interactions within a ~5-Å radius of these residues (Fig. 1h). Thus, the results of our MD simulations suggest that, in the absence of repulsive electrostatic interactions, ThT can bind to a minimal groove formed from four aromatic–hydrophobic cross-strand residues.

The remaining binding modes B, C, and D are further dominated by hydrophobic and aromatic stacking interactions. In binding mode B, ThT lies diagonally on a cross-strand Ser-Thr pair, with the benzyl ring partially buried beneath Tyr159 in a parallel-displaced manner. Binding mode C is mediated by benzathiole stacking against Tyr205, while the benzyl ring packs against Leu203. Finally, in binding mode D, the benzathiole ring and terminal methyl pack against the exposed aromatic ring of Phe126, projecting the benzyl ring into solvent.

To gain a more quantitative understanding of binding at different sites, we evaluated the binding energies of each structural superfamily using the MM-GBSA (molecular mechanics-generalized Born/surface area) method as described in the caption of Fig. 2. These energies, averaged from the representative structures shown in Fig. S2, are noted in Fig. 2. The four binding sites for ThT have binding energies ranging from ~−9.8 to ~−18.7 kcal/mol. The lowest binding energy (−18.7 kcal/mol) corresponds to binding in the groove formed by the five Tyr side chains in mode A.

Our results further support the growing body of evidence that ThT preferentially binds to surfaces created by hydrophobic and aromatic side-chain channels running perpendicular to the long-axis of

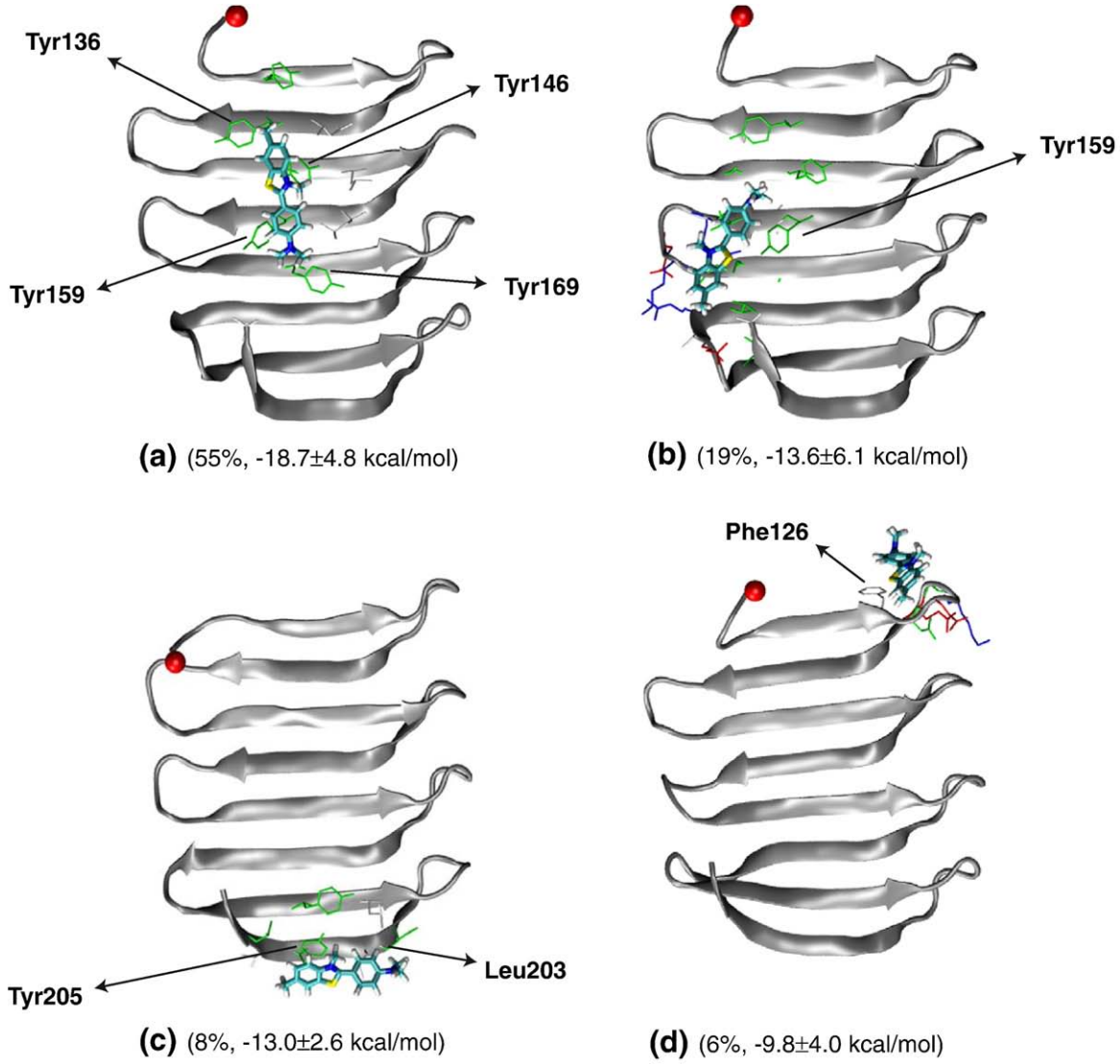

Fig. 2. Four binding sites of ThT to the SLB of the 5-YY/LL PSAM. (a) Binding on the top of five consecutive Tyr side chains across β-strands. (b) Binding on top of Ser and Thr. (c) Binding at the upper edge of the SLB. (d) Binding at the lower edge of the SLB. The abundance and MM-GBSA binding energies for each of the four structural superfamilies are noted in parentheses. The N-terminus is shown as a red ball. Only the surface side chains (blue, positively charged; red, negatively charged; black, hydrophobic) are shown. Atoms C, N, S, and H of the dye are colored cyan, blue, yellow, and white, respectively. *Binding energy calculation*: The binding energy of a dye molecule to the 5-YY/LL PSAM in each site was evaluated on the centroid of the structural superfamilies using the MM-GBSA module[17] in the AMBER package in which the solvation free energy is represented by the generalized Born term (the polar part of the solvation) and a surface area term (the apolar part of the solvation free energy). Although the MM-GBSA calculations may overestimate the absolute binding free energy due to missing entropic terms (e.g., translation, rotation, and conformational entropy change of the solute upon binding), they usually give a reasonable estimate of the relative binding free energy when the entropic change of two binding sites are comparable.[17,18]

β-sheets (as seen in binding mode A).[4,7,14,15,19] While ThT shows a clear preferred binding site (in terms of binding energy and abundance), it is capable of binding at other sites (as seen in binding modes B, C, and D). This observation is consistent with the fact that ThT is known to bind at more than one location to Aβ fibrils.[7,14,20] Moreover, although binding modes C and D (at the edge of the SLB) would not be possible in the context of the full-length PSAM protein, as the N- and C-terminal capping domains occlude these sites, these modes are relevant for fibril-like structures that contain exposed β-sheet edges.[7,14] As was seen in our earlier work on the binding of ThT to $A\beta_{16–22}$ fibrils, these modes correspond to minor binding modes by ThT in terms of both binding affinities and site density (Fig. 2).

Quantum calculations by Stsiapura *et al.* suggest that the increase in ThT fluorescence upon binding to amyloid is primarily the result of steric immobilization of ThT's two aromatic rings.[21] Binding to amyloid fibrils locks ThT in a near-planar (~37°) conformation (a fluorescent state) and prevents rotation into the twisted (~90°) conformer (a

nonfluorescent state). The energy barrier going from the near-planar to the twisted conformation is about 4 kcal/mol, and the conversion between these conformers (in the unbound state) is mainly activated at the electronically excited state with a charge transfer, favoring the twisted conformation.[21] This effect cannot be captured in the classical simulations presented in this article. The ThT molecule in our simulations is at its electronic ground state and, thus, is dominantly found in the near-planar conformation in both the unbound and bound states. We can only report here on the binding locations of ThT; not all of them necessarily will result in enhanced fluorescence. However, the fact that the primary binding mode seen in our simulations (site A) maps onto the site of the Tyr and Leu mutations used to transform the wild-type PSAM into the ThT-staining 5-YY/LL PSAM suggests that this is indeed the corresponding binding site that leads to enhanced ThT fluorescence.

In conclusion, the simulations presented here have provided detailed information about binding of ThT to the 5-YY/LL PSAM and have complemented earlier experimental work in which the location of the ThT binding site could not be directly visualized. The combined experimental and theoretical work shows that the straight and shallow groove formed by four aromatic–hydrophobic residues most likely comprises the minimal binding site for ThT in the designed PSAM. It is interesting to note that our simulations of the binding of ThT to $A\beta_{16–22}$ fibrils[14] as well as to a single peptide layer protofibril of the Alzheimer $A\beta_{9–40}$ peptide (unpublished results) also have a dominant binding mode binding to aromatic residues (Phe for $A\beta_{16–22}$ and His and Phe for $A\beta_{9–40}$) across four consecutive β-strands. Many aggregating peptides have aromatic residues[22] on the β-sheet surface (e.g., amylin[23] and Aβ peptide[24–27]), and grooves formed by these residues across consecutive β-strands may prove to be a generic recognition motif for ThT binding to fibrils. In addition, we speculate that the minimum requirement for ThT binding identified for PSAM systems can also be applied to amyloid fibrils formed from globular proteins such as β2-microglobulin[28] and transthyretin.[29] These fibrils appear to retain most of the native structure of the proteins from which they are derived. The flat β-sheet surfaces found in the native structures of these aggregating proteins are typically only three β-strands in width and would hence lead to a weak ThT binding. However, when assembled "edge to edge" in the context of the fibrils,[28,29] these proteins create extended and locally flat β-sheet surfaces. We expect that ThT can bind to grooves formed along these large β-sheets in a similar way to that proposed here for the PSAM systems.

Acknowledgements

This project is funded by the David and Lucile Packard Foundation and the National Science Foundation (MCB 0642086 and CMMI-0709079). M.B. acknowledges The Winston Churchill Foundation of the United States for support. Simulations were performed on the Lonestar cluster at the Texas Advanced Computing Center (LRAC MCA 05S027).

Supplementary Data

Supplementary data associated with this article can be found, in the online version, at doi:10.1016/j.jmb.2009.09.056

References

1. Furumoto, S., Okamura, N., Iwata, R., Yanai, K., Arai, H. & Kudo, Y. (2007). Recent advances in the development of amyloid imaging agents. *Curr. Top. Med. Chem.* **7**, 1773–1789.
2. Ban, T., Hamada, D., Hasegawa, K., Naiki, H. & Goto, Y. (2003). Direct observation of amyloid fibril growth monitored by thioflavin T fluorescence. *J. Biol. Chem.* **278**, 16462–16465.
3. Makabe, K., McElheny, D., Tereshko, V., Hilyard, A., Gawlak, G., Yan, S. *et al.* (2006). Atomic structures of peptide self-assembly mimics. *Proc. Natl Acad. Sci. USA*, **103**, 17753–17758.
4. Biancalana, M., Makabe, K., Koide, A. & Koide, S. (2009). Molecular mechanism of thioflavin-T binding to the surface of β-rich peptide self-assemblies. *J. Mol. Biol.* **385**, 1052–1063.
5. Duan, Y., Chowdhury, S., Xiong, G., Wu, C., Zhang, W., Lee, T. *et al.* (2003). A point-charge force field for molecular mechanics simulations of proteins based on condensed-phase QM calculations. *J. Comp. Chem.* **24**, 1999–2012.
6. Jorgensen, W. L., Chandrasekhar, J., Madura, J. D., Impey, R. W. & Klein, M. L. (1983). Comparisons of simple potential functions for simulating liquid water. *J. Chem. Phys.* **79**, 926–935.
7. Wu, C., Wang, Z. X., Lei, H. X., Zhang, W. & Duan, Y. (2007). Dual binding modes of Congo red to amyloid protofibril surface observed in molecular dynamics simulations. *J. Am. Chem. Soc.* **129**, 1225–1232.
8. Wang, J. M., Wolf, R. M., Caldwell, J. W., Kollman, P. A. & Case, D. A. (2004). Development and testing of a general amber force field. *J. Comp. Chem.* **25**, 1157–1174.
9. Essmann, U., Perera, L., Berkowitz, M. L., Darden, T. A., Lee, H. & Pedersen, L. G. (1995). A smooth particle mesh Ewald method. *J. Chem. Phys.* **103**, 8577–8593.
10. Ryckaert, J.-P., Ciccotti, G. & Berendsen, H. J. C. (1977). Numerical integration of the Cartesian equations of motion of a system with constraints: molecular dynamics of *n*-alkanes. *J. Chem. Phys.* **23**, 327–341.
11. Procacci, P. & Berne, B. J. (1994). Multiple time scale methods for constant pressure molecular dynamics simulations of molecular systems. *Mol. Phys.* **83**, 255–272.
12. Chiu, S. W., Clark, M., Subramaniam, S. & Jakobsson, E. (2000). Collective motion artifacts arising in long-duration molecular dynamics simulations. *J. Comp. Chem.* **21**, 121–131.
13. Harvey, S. C., Tan, R. K. Z. & Cheatham, T. E. (1998). The flying ice cube: velocity rescaling in molecular

dynamics leads to violation of energy equipartition. *J. Comp. Chem.* **19**, 726–740.
14. Wu, C., Wang, Z. X., Lei, H. X., Duan, Y., Bowers, M. T. & Shea, J. E. (2008). The binding of thioflavin T and its neutral analog BTA-1 to protofibrils of the Alzheimer's disease Aβ(16–22) peptide probed by molecular dynamics simulations. *J. Mol. Biol.* **384**, 718–729.
15. Krebs, M. R. H., Bromley, E. H. C. & Donald, A. M. (2005). The binding of thioflavin-T to amyloid fibrils: localisation and implications. *J. Struct. Biol.* **149**, 30–37.
16. Wu, C., Lei, H., Wang, Z. X., Zhang, W. & Duan, Y. (2006). Phenol red interacts with the protofibril-like oligomers of an amyloidogenic hexapeptide NFGAIL through both hydrophobic and aromatic contacts. *Biophys. J.* **91**, 3664–3672.
17. Kollman, P. A., Massova, I., Reyes, C., Kuhn, B., Huo, S., Chong, L. *et al.* (2000). Calculating structures and free energies of complex molecules: combining molecular mechanics and continuum models. *Acc. Chem. Res.* **33**, 889–897.
18. Gilson, M. K. & Zhou, H. X. (2007). Calculation of protein–ligand binding affinities. *Annu. Rev. Biophys. Biomol. Struct.* **36**, 21–42.
19. Groenning, M. (2009). Binding mode of thioflavin T and other molecular probes in the context of amyloid fibrils—current status. *J. Chem. Biol.*; published online.
20. Lockhart, A., Ye, L., Judd, D. B., Merritt, A. T., Lowe, P. N., Morgenstern, J. L. *et al.* (2005). Evidence for the presence of three distinct binding sites for the thioflavin T class of Alzheimer's disease PET imaging agents on β-amyloid peptide fibrils. *J. Biol. Chem.* **280**, 7677–7684.
21. Stsiapura, V. I., Maskevich, A. A., Kuzmitsky, V. A., Turoverov, K. K. & Kuznetsova, I. M. (2007). Computational study of thioflavin T torsional relaxation in the excited state. *J. Phys. Chem. A*, **111**, 4829–4835.
22. Gazit, E. (2005). Mechanisms of amyloid fibril self-assembly and inhibition. *FEBS J.* **272**, 5971–5978.
23. Luca, S., Yau, W. M., Leapman, R. & Tycko, R. (2007). Peptide conformation and supramolecular organization in amylin fibrils: constraints from solid-state NMR. *Biochemistry (Moscow)*, **46**, 13505–13522.
24. Ma, B. Y. & Nussinov, R. (2002). Stabilities and conformations of Alzheimer's β-amyloid peptide oligomers (Aβ(16–22), Aβ(16–35) and Aβ(10–35)): sequence effects. *Proc. Natl Acad. Sci. USA*, **99**, 14126–14131.
25. Petkova, A. T., Ishii, Y., Balbach, J. J., Antzutkin, O. N., Leapman, R. D., Delaglio, F. & Tycko, R. (2002). A structural model for Alzheimer's β-amyloid fibrils based on experimental constraints from solid state NMR. *Proc. Natl Acad. Sci. USA*, **99**, 16742–16747.
26. Buchete, N. V., Tycko, R. & Hummer, G. (2005). Molecular dynamics simulations of Alzheimer's β-amyloid protofilaments. *J. Mol. Biol.* **353**, 804–821.
27. Buchete, N. V. & Hummer, G. (2007). Structure and dynamics of parallel beta-sheets, hydrophobic core, and loops in Alzheimer's A beta fibrils. *Biophys. J.* **92**, 3032–3039.
28. Benyamini, H., Gunasekaran, K., Wolfson, H. & Nussinov, R. (2003). Beta(2)-microglobulin amyloidosis: insights from conservation analysis and fibril modelling by protein docking techniques. *J. Mol. Biol.* **330**, 159–174.
29. Serag, A. A., Altenbach, C., Gingery, M., Hubbell, W. L. & Yeates, T. O. (2002). Arrangement of subunits and ordering of beta-strands in an amyloid sheet. *Nat. Struct. Biol.* **9**, 734–739.